Journal of Engineering and Technology for Industrial Applications

ISSN ONLINE: 2447-0228

ITEGAM-JETIA

Manaus, v.12 n.57, p. 01-15. January/February, 2026.

DOI: https://doi.org/10.5935/jetia. v12i57.2372

RESEARCH ARTICLE OPEN ACCESS

INTELLIGENT CONTROL STRATEGIES FOR DFIG-BASED WIND ENERGY SYSTEMS: A COMPARATIVE ANALYSIS OF TYPE-1 FUZZY, INTERVAL TYPE-2 FUZZY, AND ANN APPROACHES

Kouadria Selman[1], Kouadria Mohamed Abdeldjabbar[2], Berkouk El Madji[3] and Rizoug Nassim[4]

[1]LGEP, Laboratoire de Génie électrique et des plasmas, Université Ibn Khaldoun, Tiaret, Algeria
[2]L2GEGI, Laboratoire de Génie Energétique et Génie Informatique, Université Ibn Khaldoun, Tiaret, Algeria
[3]LCP, Laboratoire de Commande des Processus, Ecole Nationale Polytechnique Algiers, Algeria
[4]ESTACA'Lab, Campus Ouest Parc Universitaire Laval-Changé, France.

[1]https://orcid.org/0000-0001-7179-2146, [2]http://orcid.org/0000-0002-5001-4131
[3]http://orcid.org/0000-0001-9558-2784, [4]http://orcid.org/0000-0002-2151-185X

Email: kouadria.selman@univ-tiaret.dz, mohamedabdeldjabbar.kouadria@univ-mosta.dz, emberkouk@yahoo.fr, nassim.rizoug@estaca.fr

ARTICLE INFO

Article History
Received: July 15, 2025
Revised: November 20, 2025
Accepted: January 1, 2026
Published: January 31, 2026

Keywords:
wind energy conversion system (WECS),
doubly fed induction generator (DFIG),
Type-1 Fuzzy Logic Control (T1FLC),
Interval Type-2 Fuzzy Logic Control (IT2FLC),
Artificial Neural Networks (ANN).

ABSTRACT

In this study, we investigate and compare three advanced control strategies, Type-1 Fuzzy Logic Control (T1FLC), Interval Type-2 Fuzzy Logic Control (IT2FLC), and Artificial Neural Networks (ANN), applied to Doubly-Fed Induction Generators (DFIGs) in Wind Energy Conversion Systems (WECS). As wind energy plays an increasingly critical role in renewable power generation, efficient and robust control of DFIGs is essential to ensure grid stability, reliability, and optimal energy extraction under variable wind conditions. T1FLC offers simplicity and robustness but may suffer from limited adaptability. IT2FLC improves upon this by managing higher levels of uncertainty and noise through the use of fuzzy sets with an additional degree of freedom. ANN-based control, on the other hand, leverages data-driven learning and non-linear mapping to achieve high performance but may require significant training and tuning. Simulations conducted in MATLAB/Simulink evaluate the performance of each controller under dynamic wind profiles, measuring key metrics such as rotor speed regulation, electromagnetic torque response, and power output stability. This comparative study provides insights for selecting suitable control schemes for DFIG-based wind energy systems under varying operational conditions.

I. INTRODUCTION

The increasing global focus on sustainable energy solutions has made wind energy a key part of the renewable energy shift. Known for being environmentally friendly, cost-effective, and abundant, wind power plays a major role in decreasing reliance on fossil fuels and reducing greenhouse gas emissions. At the heart of this change are Wind Energy Conversion Systems (WECS), especially those using Doubly-Fed Induction Generators (DFIGs), which provide better control, higher energy efficiency, and flexibility to adapt to changing wind conditions [1], [2]. DFIG-based Wind Energy Conversion Systems (WECS) are widely adopted due to their ability to operate effectively over a wide range of speeds, maximizing power output through advanced control methods like Maximum Power Point Tracking (MPPT). Unlike fixed-speed systems, variable-speed DFIG systems allow for real-time adjustments to rotor speed, boosting energy capture and reducing mechanical stress. However, controlling DFIGs is difficult because of their nonlinear dynamics, the coupling between control variables, and their sensitivity to parameter changes and external disturbances. [3], [4]. To address these challenges, researchers have shifted away from traditional control strategies like Proportional-Integral (PI) controllers. Although these are simple and commonly used, they often lack robustness in uncertain and variable operating conditions. Consequently, there has been a rise in intelligent control methods that can more effectively handle the dynamic and nonlinear characteristics of wind energy systems [5], [6].

Among these, Type-1 Fuzzy Logic Controllers (T1-FLCs) offer improved adaptability by incorporating linguistic rules and expert knowledge to handle system nonlinearities without requiring precise mathematical models. However, their performance can degrade in the presence of significant uncertainties. To address this, Interval Type-2 Fuzzy Logic Controllers (IT2-FLCs) have been developed, extending the fuzzy logic paradigm by modeling uncertainties within membership functions using a Footprint of Uncertainty (FOU). This allows IT2-FLCs to provide enhanced robustness and tracking performance under turbulent wind conditions and parameter variations [7-9]. Parallel to fuzzy logic approaches, Artificial Neural Networks (ANNs) have emerged as a powerful tool for intelligent control. Leveraging their ability to learn complex nonlinear mappings from data, ANNs can adapt to changing dynamics without explicit system modeling, making them highly suitable for unpredictable environments.

However, their effectiveness is closely tied to the quality of training data and the computational resources available [10], [11]. This study presents a comparative analysis of three advanced intelligent control strategies, Type-1 FLC, Interval Type-2 FLC, and ANN applied to DFIG-based wind energy systems. The objective is to evaluate each controller's performance in terms of robustness, tracking accuracy, and computational efficiency under variable wind and system conditions. Through this analysis, the paper aims to identify optimal control methodologies that can enhance the reliability and efficiency of modern wind energy systems, supporting their broader integration into the power grid. Figure 1 illustrates the global scheme of the proposed control strategy, in which three types of controllers are investigated: Type-1 fuzzy logic controller (T1-FLC), Interval type-2 fuzzy logic controller (IT2-FLC), and artificial neural network (ANN) controller.

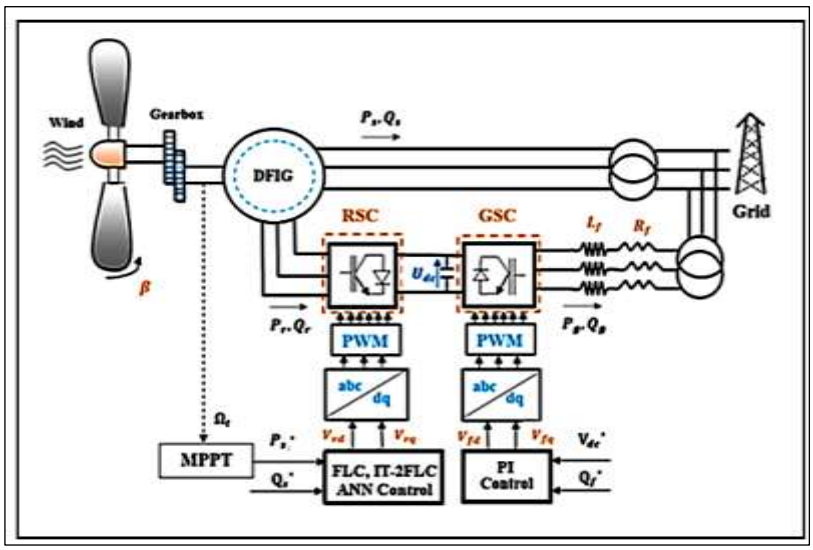

Figure 1: Wind Energy Conversion System configuration.
Source: Authors, (2026).

This paper is structured into six sections. Section 1 provides an overview of wind energy conversion systems and highlights the motivation for applying intelligent control strategies in Doubly-Fed Induction Generator (DFIG)-based systems. Sections 2 and 3 present the modeling of the wind turbine and describe the implementation of a Maximum Power Point Tracking (MPPT) algorithm, respectively. Section 4 focuses on the mathematical modeling of the DFIG. Section 5 presents the simulation results under various operating conditions to evaluate and compare the performance of Type-1 Fuzzy Logic Control (T1-FLC), Interval Type-2 Fuzzy Logic Control (IT2-FLC), and Artificial Neural Network (ANN)-based control strategies. Finally, Section 6 concludes the paper with a summary of the key findings and recommendations for future research.

II. MODELING OF THE WIND GENERATOR

II.1 MODEL Of WIND TURBINE

The wind turbine is the core component of a WECS, and its mechanical power output is determined by its aerodynamic properties as described by the following formula [4],[5],[12].

$$P_w = \frac{1}{2}\rho\pi R^2 v_t^3 C_P(\lambda,\beta) \tag{1}$$

Where:

$$\lambda = \frac{\omega_t . R}{v_t} \tag{2}$$

The aerodynamic torque is commonly represented as follows[13]:

$$T_w = \frac{1}{2}\frac{\rho.\pi.R^3.v_t^2.C_P(\lambda,\beta)}{\lambda} \tag{3}$$

A fundamental equation is used to represent $C_P(\beta,\lambda)$, which is derived from the aerodynamic characteristics of the turbine [13-16]:

$$C_p\left(\lambda,\beta\right)=0.5176.\left(116.\frac{1}{\lambda_i}-0.4.\beta-5\right)e^{-\frac{21}{\lambda_i}}+0.0068.\lambda \tag{4}$$

With

$$\frac{1}{\lambda_i}=\frac{1}{0.08.\beta+\lambda}-\frac{0.035}{1+\beta^3} \tag{5}$$

II.2 MAXIMUM POWER POINT TRACKING TECHNIQUE

MPPT strategies are essential for maximizing power extraction in WECS and improving efficiency. Two main approaches exist: with or without speed control. This discussion focuses on speed control-based MPPT, which regulates turbine rotation to optimize power extraction [4], [5]. Maximum power is achieved when C_P reaches its highest value at a specific λ , corresponding to an optimal rotor speed for each wind speed. However, wind variability can cause deviations from this optimal point, leading to energy losses. An MPPT system continuously optimizes energy transfer to the grid to mitigate these losses [17].

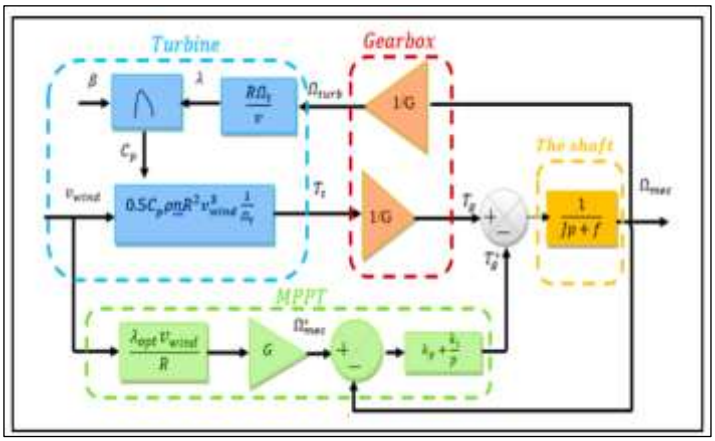

Figure 2: Diagram block of the MPPT extracted with speed control.
Source: Authors, (2026).

The $C_{P\max}=0.48$ is attained when the $\beta=0$ and $\lambda=8.12$ .To sustain this condition, the reference electromagnetic torque is maximized using the given equation [4], [17]:

$$T_{em-ref}=\frac{1}{2}\frac{\rho\pi R_t^5 C_{p\max}}{\lambda_{opt}^3 G^3}\Omega_{mec}^2 \tag{6}$$

Figure 3 presents the $C_P(\beta,\lambda)$ characteristics corresponding to various pitch angle values β [12].

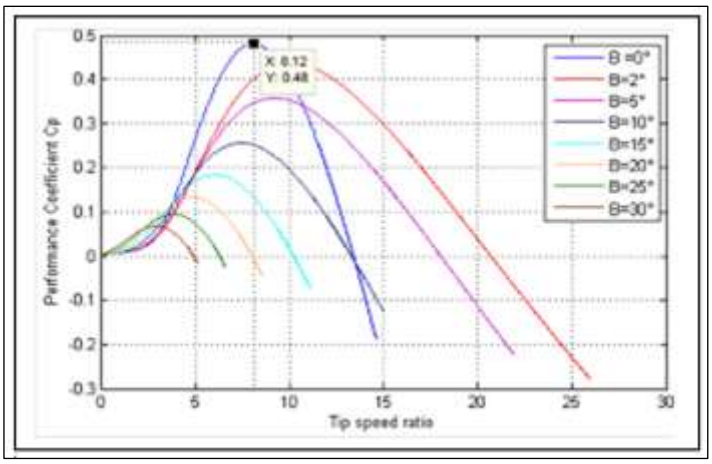

Figure 3: The typical performance coefficient curve.
Source: Authors, (2026).

II.3 DFIG MATHEMATICAL MODELING

The DFIG model is developed using Park's transformation [3-5], [18]. The voltage Equations:

$$\begin{cases} V_{qs} = \dfrac{d\varphi_{qs}}{dt} + R_s I_{qs} - \omega_s \varphi_{ds} \\ V_{ds} = \dfrac{d\varphi_{ds}}{dt} + R_s I_{ds} - \omega_s \varphi_{qs} \\ V_{qr} = \dfrac{d\varphi_{qr}}{dt} + R_r I_{qr} - (\omega_s - \omega_r)\varphi_{dr} \\ V_{dr} = \dfrac{d\varphi_{dr}}{dt} + R_r I_{dr} - (\omega_s - \omega_r)\varphi_{qr} \end{cases} \tag{7}$$

Flux Equations:

$$\begin{cases} \varphi_{ds} = L_m I_{dr} + L_s I_{ds} \\ \varphi_{qs} = L_m I_{qr} + L_s I_{qs} \\ \varphi_{dr} = L_m I_{ds} + L_r I_{dr} \\ \varphi_{qr} = L_m I_{qs} + L_r I_{qr} \end{cases} \tag{8}$$

DFIG electromagnetic torque is:

$$T_{em} = \frac{3}{2} p\left(\varphi_{ds} I_{qs} - \varphi_{qs} I_{ds}\right) \tag{9}$$

P_S and Q_S are determined by:

$$\begin{cases} P_s = \dfrac{3}{2}\left(V_{ds} I_{ds} + V_{qs} I_{qs}\right) \\ Q_s = \dfrac{3}{2}\left(V_{qs} I_{ds} - V_{ds} I_{qs}\right) \end{cases} \tag{10}$$

II.4 DFIG MODEL WITH STATOR FLUX ORIENTATION

The RSC operates in a synchronous reference system with a d-axis aligned to the stator flux, allowing independent control of P and Q power [18]:

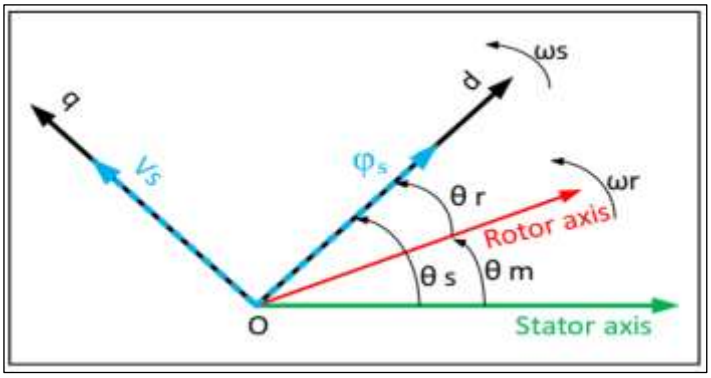

Figure 4: Orientation of the d, q frame.
Source: Authors, (2026).

$$\begin{cases} \varphi_{ds} = \varphi_s \\ \dfrac{d\varphi_{qs}}{dt} = \varphi_{qs} = 0 \end{cases} \tag{11}$$

Apply the following criteria to get the simplified equation for electromagnetic torque:

As a result, we get

$$T_{em} = \frac{3}{2} p \varphi_s I_{qs} \tag{12}$$

Assuming the R_S is ignored, the voltage and flux equations simplify to:

$$\begin{cases} V_{ds} = 0 \\ V_{qs} = \omega_s \varphi_{ds} \end{cases} \tag{13}$$

$$\begin{cases} \varphi_s = L_s I_{ds} + L_m I_{dr} \\ 0 = L_s I_{qs} + L_m I_{qr} \end{cases} \tag{14}$$

Equation (14) defines the correlation between stator and rotor currents.

$$\begin{cases} I_{ds} = \dfrac{\varphi_s}{L_s} - \dfrac{L_m}{L_s} I_{dr} \\ I_{qs} = -\dfrac{L_m}{L_s} I_{qr} \end{cases} \tag{15}$$

P_S and Q_S are given by:

$$\begin{cases} P_s = \dfrac{3}{2} V_s I_{qs} \\ Q_s = \dfrac{3}{2} V_s I_{ds} \end{cases} \tag{16}$$

The electromagnetic torque is determined by integrating equations (12) and (15):

$$T_{em} = -\frac{3}{2} p \frac{L_m}{L_s} \varphi_s I_{qr} \tag{17}$$

By substituting the expressions for the stator currents found in (15), the power equations can be expressed in the following form:

$$\begin{cases} P_s = -\dfrac{3}{2} V_s \dfrac{L_m}{L_s} I_{qr} \\ Q_s = \dfrac{3}{2} V_s \left(\dfrac{\varphi_s}{L_s} - \dfrac{L_m}{L_s} I_{dr} \right) \end{cases} \tag{18}$$

The voltage equations can be represented as follows:

$$\begin{cases} V_{dr} = R_r I_{dr} - g\omega_s \left(L_r - \dfrac{L_m^2}{L_s} \right) I_{qr} \\ V_{qr} = R_r I_{qr} + g\omega_s \left(L_r - \dfrac{L^2_m}{L_s} \right) I_{dr} + g \dfrac{L_m V_s}{L_s} \end{cases} \tag{19}$$

III. INTELLIGENT CONTROL STRATEGIES

III.1 DESCRIPTION OF FUZZY LOGIC SETS

To address the limitations of classical control methods, particularly their reduced performance when actual machine parameters differ from those assumed in the control design, we chose to implement a fuzzy logic controller to manage the behavior of the DFIG wind turbine, focusing primarily on regulating active and reactive power [8].

III.1.1 Overview of Type-1 Fuzzy Logic Sets (T1-Fls)

For any element x within a universe X, a type-1 fuzzy set assigns a membership degree, between 0 and 1, to that element using a function $\mu_A(x)$. We can therefore represent a type-1 fuzzy set as a collection of ordered pairs, where each pair consists of an element and its associated membership degree, as precisely defined by Equation (20). [7-10]:

$$A = \left(x, \mu_A(x) \right) \middle| \forall x \in X \tag{20}$$

Where

$$\mu_A : X \to [0,1]$$

In this definition, $\mu_A(x)$ represents the membership degree of the element $x \in X$ to the set A. In this work, the following notation is used:

$$A(x) = \mu_A(x) \tag{21}$$

For all $x \in X$.

III.1.2 Control of Doubly Fed Induction Generator Using T1-Flc

Figure 5 illustrates the DFIG-based Wind Energy Conversion (WEC) system model simulated using a conventional Type-1 Fuzzy Logic Controller (T1-FLC). Two control loops are presented:

The power control loop regulates the active and reactive power by generating the reference rotor current components I_{rq}^{*} and I_{rd}^{*}, respectively. It employs Type-1 Fuzzy Logic Controllers (T1-FLCs) that process the power errors and their rate of change to provide smooth and adaptive control responses. The current control loop ensures that the actual rotor current components follow the generated references. It also utilizes T1-FLCs to compute the appropriate voltage signals for the rotor-side converter.

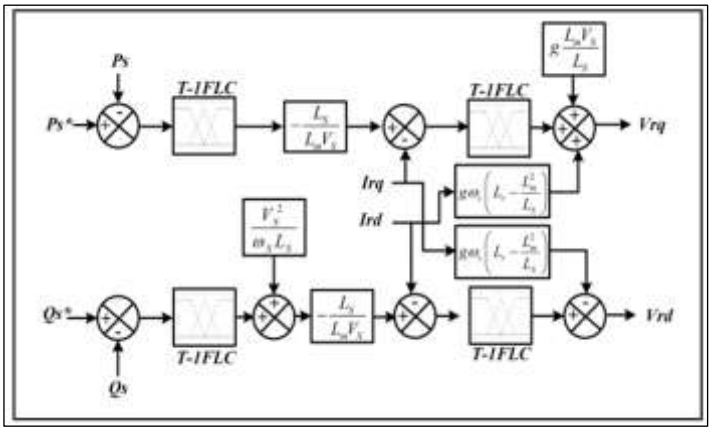

Figure 5: Block diagram illustrating the structure of a type-1 fuzzy logic controller.
Source: Authors, (2026).

III.1.3 Basic Concepts of Interval Type-2 Fuzzy Logic Sets (It-2fls)

According to the definition of Zadeh, A type-2 fuzzy sets are the generalized forms of type-1 fuzzy sets. An interval type-2 fuzzy set, denoted as $\tilde{\tilde{A}}$, is characterized by a type-2 membership function $\mu_{\tilde{\tilde{A}}}(x,u)$ and can be described as [7],[8],[14]-[16],[18]-[22]:

$$\tilde{\tilde{A}} = \left\{ (x,u), \mu_{\tilde{\tilde{A}}}(x,u) \right\} \left| \forall x \in X, \forall u \in J_x^u \subseteq [0,1] \right. \tag{22}$$

In which

$$x \in X, u \in J_x^u \subseteq [0,1] \text{ and } \quad 0 \le \mu_{\tilde{\tilde{A}}}(x,u) \le 1$$

$\left(\tilde{\tilde{A}}\right)$ can be also expressed as:

$$\tilde{\tilde{A}} = \int_{x \in X} \int_{u \in Jx} \mu_{\tilde{\tilde{A}}}(x,u) / (x,u), Jx \subseteq [0,1] \tag{23}$$

Where $\int_{x \in X} \int_{u \in Jx}$ denote union over all admissible input variables x and u.

Here, X is the primary domain of the input variable, x is the value of the input variable, u is the primary grade of a type-2 fuzzy set, and J_x is called the primary membership of a type-2 fuzzy set of x and $\mu_{\tilde{\tilde{A}}}(x,u)$ is the secondary membership function equal to 1.

Another expression for $\left(\tilde{\tilde{A}}\right)$ is:

$$\tilde{\tilde{A}} = \int_{x \in X} \int_{u \in Jx} 1 / (x,u), Jx \subseteq [0,1] \tag{24}$$

$$\tilde{\tilde{A}} : X \to \left\{ [a,b] : 0 \le a \le b \le 1 \right\}$$

The union of all the primary memberships represents the uncertainty about $\left(\tilde{\tilde{A}}\right)$, which is called the footprint of uncertainty (Fou) of $\left(\tilde{\tilde{A}}\right)$ as shown in Figure 3, i.e., [7],[8].

$$Fou\left(\tilde{\tilde{A}}\right) = U_{\forall \in X} J_x = \left\{ (x,u) : u \in J_x \subseteq [0,1] \right\} \tag{25}$$

The (Fou) of $\left(\tilde{\tilde{A}}\right)$ is bounded by two type-1 MFs called upper membership function (UMF) and lower membership function (LMF) as shown in Figure 6. The LMF and UMF are denoted as $\underline{\mu}_{\tilde{\tilde{A}}}(x)$ and $\overline{\mu}_{\tilde{\tilde{A}}}(x)$, respectively, and are defined as follows:

$$\underline{\mu}_{\tilde{A}}(x) = \underline{Fou\left(\tilde{A}\right)}, \forall x \in X \tag{26}$$

$$\overline{\mu}_{\tilde{A}}(x) = \overline{Fou\left(\tilde{A}\right)}, \forall x \in X \tag{27}$$

Note that J_x is an interval set; i.e.,

$$Jx = \left\{(x,u) : u \in \left[\overline{\mu}_{\tilde{A}}(x), \underline{\mu}_{\tilde{A}}(x)\right]\right\} \tag{28}$$

An embedded fuzzy set $\left(\tilde{A}_e\right)$ for a continuous universe of discourse x and u is described as

$$\left(\tilde{A}_e\right) = \int_{x \in X}\left(\frac{[1/u]}{x}\right), u \in J_x \tag{29}$$

The set $\left(\tilde{A}_e\right)$ is embedded in $\left(\tilde{A}\right)$ in such a way that the secondary membership functions (MFs) are always one at each value of x . A large number of such embedded type-1 fuzzy sets (T1-FSs) are combined to form the type-2 fuzzy set (T2-FS), which enables the detailed description of the analytical control surface; the addition of the extra levels of classification gives a much smoother control surface and response. The T2-FS can be considered as a combination of many different type-1 fuzzy sets where each (T1-FS) is embedded to form the (Fou) [7-10],[14],[16].

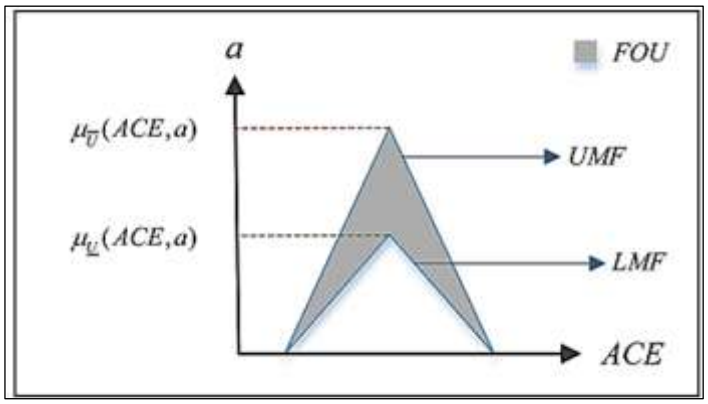

Figure 6: Type-2 fuzzy set with FOU and embedded FS.
Source: [9].

III.1.4 Control of Doubly Fed Induction Generator Using It2-Flc

The Interval type-2 fuzzy logic controller (IT2-FLC) is very useful in circumstances where we need to take into consideration the different uncertainties as the real machine parameters change, and as the controller for a variable speed wind turbine-based on DFIG is used mainly to regulate active and reactive power exchanged with an electrical network. To control a DFIG-based wind energy conversion system easily, we used the independent control of active and reactive power using the stator flux orientation. In the control diagram, the classical rotor currents controllers were replaced by an IT 2-FLC [8],[16].

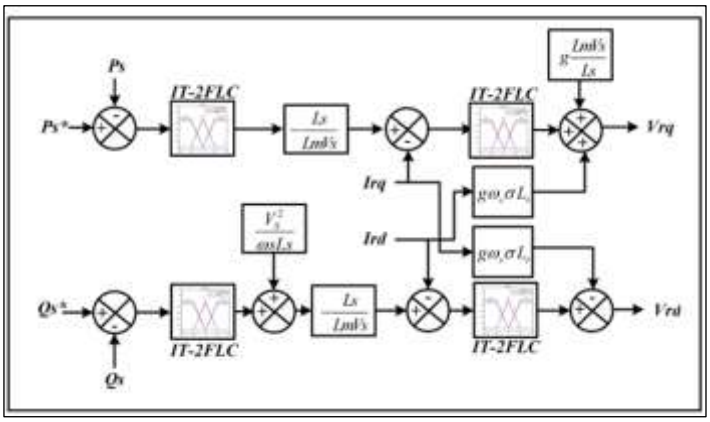

Figure 7: Block diagram illustrating the structure of an Interval type-2 fuzzy logic controller.
Source: Authors, (2026).

The DFIG-based WEC system model was simulated first using a conventional T1-FLC (Figure 5) and then an IT2-FLC. The rule base was the same for both type-1 and type-2 fuzzy logic controllers. The fuzzy control strategy is based on a human operator's experience to interpret a situation and initiate its control action. The scheme of the control of the DFIG-based WEC system using an IT2-FLC is presented in Figure 7.

The core of the type-2 fuzzy logic controller (IT2-FLC) is the type-1 fuzzy logic controller (T1-FLC), as Figure 8 shows. The IT2-FLC is constituted of four functional blocks, the three blocks of type-1 fuzzy and a fourth functional block that ensures the type reducer transforms a type-2 fuzzy set into a type-1 fuzzy set [16]. The structures of IT2-FLS and T1-FLS are shown in Figure 4a and b, respectively [7],[8],[14-16],[19],[20]. The fuzzifier stage is used to translate inputs (real values) to fuzzy values. The inference (reasoning) stage consists of two blocks, the rules base and the inference engine; it works the same way as for type-1 fuzzy systems, except the antecedents' fuzzy sets and the consequent are represented by type-2 fuzzy sets. The process consists of combining the rules base to produce a mapping from input to the output type-2 fuzzy set [7]. It is necessary to calculate the intersection, union and composition of type-2 relations in order to realize this mapping. The type reducer is used to convert all type-2 fuzzy sets into a type-1 fuzzy set on the output. There are several methods to calculate the reduced set, such as joint center, center of sums, height, and center joint, among others [8]. The defuzzification stage translates an output into precise values. A comparison between a T1-FLC and an IT2-FLC is given in the following.

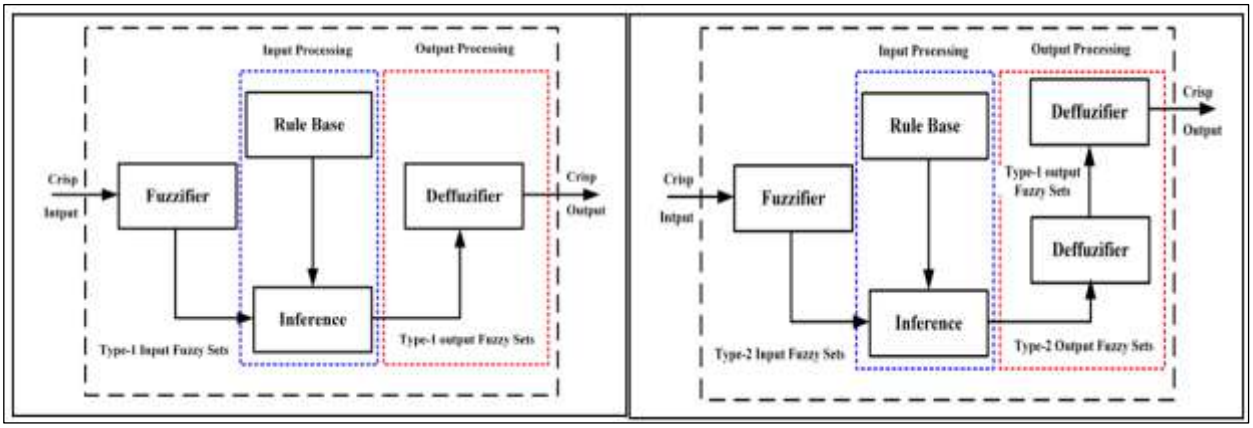

Figure 8: Structures of fuzzy logic control: (a)Type-1 fuzzy logic controller (T1-FLC);
(b) interval type 2 fuzzy logic controller (IT2-FLC).
Source: Authors, (2026).

In this paper, three triangular membership functions were chosen for the IT2-FLC and T1-FLC, because these membership functions are easier to implement in practical hardware, used as the inputs and outputs, which are also shown in Figures 9 and 10, respectively. The maximum and minimum values of the universe of discourse for all inputs and outputs are -1 to +1 [8].]

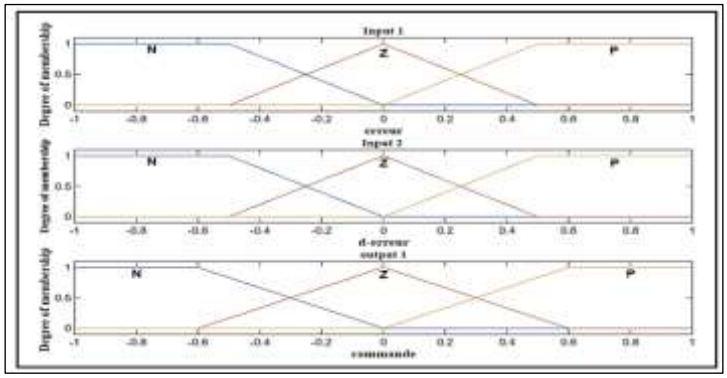

Figure 9: Type-1 fuzzy membership functions (MFs):
MFs corresponding to the input variables 'e' (error)
and 'de' (change in error), as well as the output
variable 'u' of the T1-FLC.
Source: Authors, (2026).

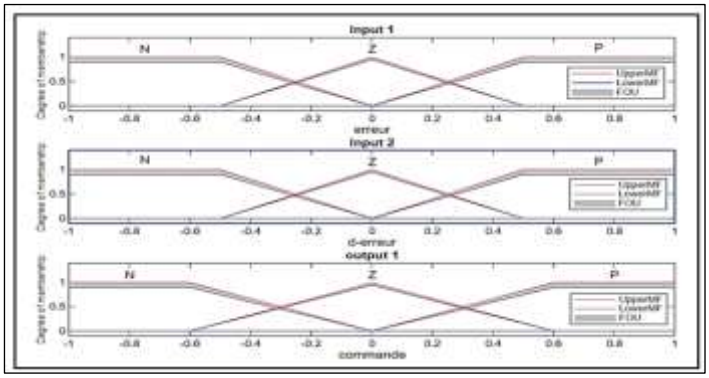

Figure 10: Interval Type-2 fuzzy membership functions (MFs):
MFs corresponding to the input variables 'e' (error)
and 'de' (change in error), as well as the output
variable 'u' of the IT2-FLC.
Source: Authors, (2026).

The controller inputs are error (e) and its derivative (de). The only output of the controller is the control signal (u). Each input and output contain three membership functions, two trapezoidal and one triangular [19]. Input and output membership functions (MFs) of the T1-FLC and IT2-FLC are demonstrated in Figures 5 and 6, respectively. For the optimal performance of the controllers, a 9-rule base was designed for the T1-FLC and IT2-FLC, as shown in Table 1. Referring to this table, N defines the negative. Z is zero while P is positive. The rule base is the core part of the T1-FLC and IT2-FLC design, which is based on process dynamics, experts' knowledge, and experience [23].

Table 1: Fuzzy logic rules.

de / e	N	Z	P
N	N	N	Z
Z	N	Z	P
P	Z	P	P

Source: Authors (2026).

The IT2-FLC was modeled on the MATLAB environment as depicted in Figure 11, and the parameters of the type-2 fuzzy (k1, k2, k3) were determined by the trial-and-error method [7].

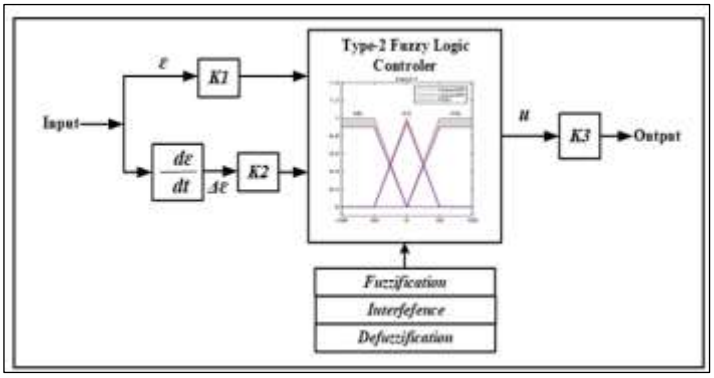

Figure 11: Schematic diagram for the IT2-FLC technique.
Source: Authors, (2026).

III.2. ARTIFICIAL NEURAL NETWORK STRATEGY FOR THE DFIG

An artificial neural network (ANN) is a computational model, inspired by the human brain, made up of interconnected processing units called neurons. These connections have adjustable weights, and each neuron uses an activation function to introduce non-linear behavior. This structure allows the network to learn complex relationships between inputs and outputs. It does this by performing two basic steps: calculating a weighted sum of its inputs and then applying a non-linear activation function to that sum [10],[11].

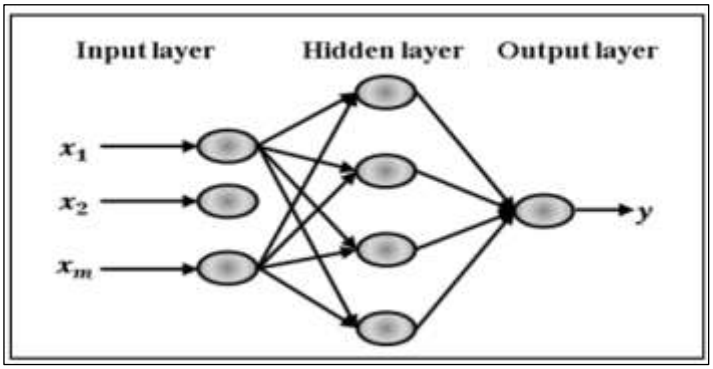

Figure12: Schematic representation of a multilayer Neural Network.
Source [10].

The inherent characteristics of Artificial Neural Networks (ANNs), including parallel processing, learning, and generalization, have established them over the last few decades as one of the most powerful methods for estimation within control systems in various applications. [24], [25]. The following functions represent the operation of the neural network:

$$y = \sum_{k=1}^{n} w_k^2 g\left(\sum_{j=1}^{p} w_{kj}^1 \varphi_j + b_k^1 \right) + b^2 \tag{30}$$

With:

φ_j : ANN input

w_{kj}^1 et b_k^1 : The weights and the bias of the hidden layer

$$g(x) = \frac{2}{1+e^{-2x}} - 1 \tag{31}$$

$g(x)$: The sigmoid function

w_k^2 et b^2 : The weights and the bias of the hidden layer

To take advantage of its advantages, an ANN is proposed in this article to simplify and improve the vector control scheme of the DFIG. The proposed ANN is used to replace the four FLC regulators (T1-FLC and IT2-FLC) in Fig. 4. For the learning of the ANN, it is done offline using a database obtained from the standard vector control diagram. To do this, the inputs and outputs of the FLC controllers are read during the simulation of the vector control for different operating conditions. Then, these data are processed to select a learning base of an appropriate size to ensure a compromise between the sought accuracy and the learning and computing time [26],[27]. Learning is done using the famous retro-propagation algorithm.

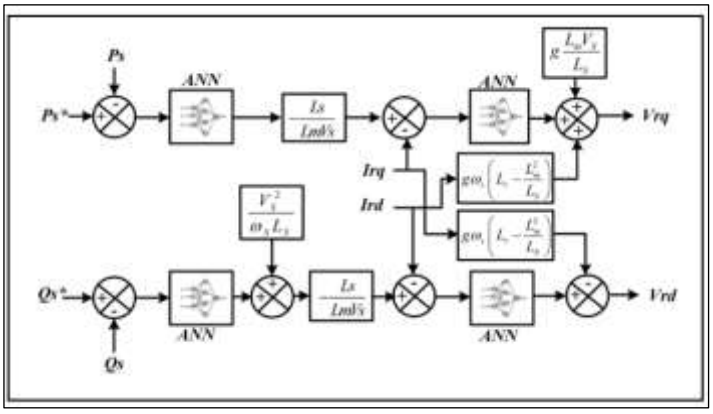

Figure 13: Block diagram illustrating the structure of Interval type-2 fuzzy logic controller.
Source: Authors, (2026).

IV. RESULTS AND DISCUSSIONS

The WECS model utilized in these simulations is based on a 10-kW wind turbine and a 7.5 kW DFIG connected to the grid, and it is implemented in the MATLAB/Simulink environment. The values of the parameters used in the models are listed in the appendix. Figure (14-a) depicts the wind speed profile employed in these simulations. Figures (14-c) and (14-d) show the highest power coefficient $C_{p\max} = 0.48$ and the maximum tip speed ratio $\lambda = 8.12$, for the simulated wind turbine model. The waveforms of optimum angular speed Ω_{opt} and observed angular rotor speed Ω_m of the DFIG are shown in Figure (14-b). The MPPT algorithm determines the reference angular rotor speed Ω_{opt}.

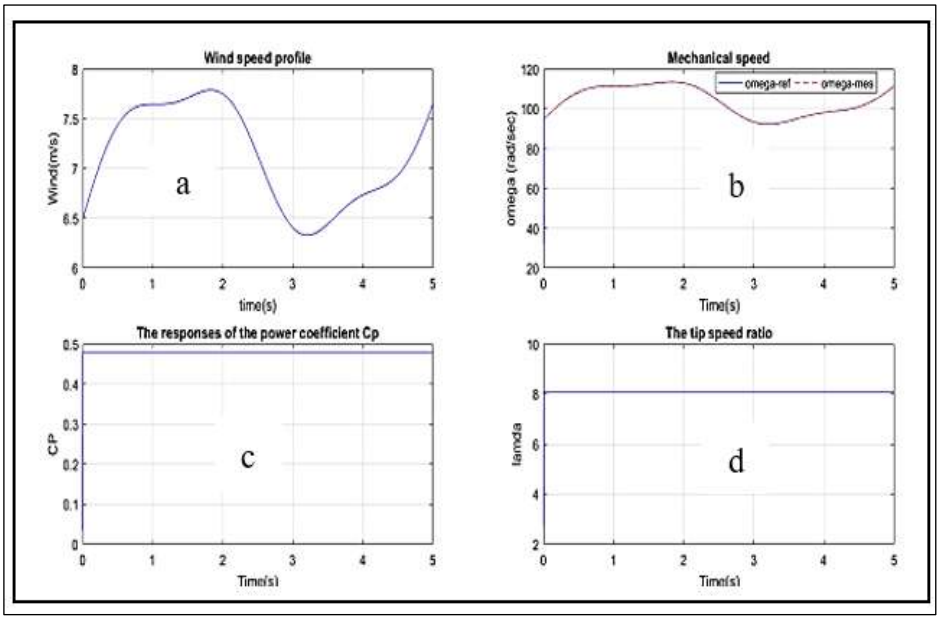

Figure 14: Wind turbine characteristics: (a) Wind speed profile, (b) Mechanical speed, (c) Power Coefficient (Cp), (d) Tip speed ratio (λ).
Source: Authors, (2026).

The simulation results shown in Figures 15, 16, and 17 depict respectively the behavior of the DFIG system under the control of three different intelligent controllers: T1-FLC, IT2-FLC, and ANN. These controllers are used to regulate the active and reactive power generated at the stator, and the control strategy allows for the decoupling of active and reactive power expressions, or equivalently, flux and torque. The simulation confirms that the stator flux follows the reference axis (d) with nearly zero quadrature components, indicating effective decoupling of the machine. The quadrature rotor current (Irq) governs the electromagnetic torque and active power, while the direct rotor current (Ird) manages reactive power exchanged between the stator and the grid. The behavior of these currents directly reflects active and reactive power dynamics, with torque responding rapidly to power demands. Comparatively, T1-FLC demonstrates a moderate transient response with an initial active power spike of approximately (6000 W) and a settling time of (9 ms).

The rotor quadrature current peaks at (20 A) and stabilizes quickly, while the direct current dips to (-20 A) before aligning with its reference of (-15 A) at (0.5 ms). The reactive power shows a dip to (-1000 VAR) and stabilizes to (0 VAR) by (0.7ms), indicating effective voltage support. IT2-FLC, in contrast, exhibits the fastest dynamic performance, with a sharper active power spike (around 16,000 W) but the shortest settling time (around 6 ms). This comes at the cost of a higher (Irq) peak (50 A), showing a more aggressive control effort. The reactive power and (Ird) behaviors are similar to T1-FLC, with stabilization occurring quickly after transients. The ANN controller offers a compromise between these two approaches. It experiences a smaller active power spike (around 8000 W) but with a slower settling time (around 14 ms).

The peak in (Irq) reaches (23.5 A), and (Ird) stabilizes at (-15 A) by (0.4 ms), showing effective control. The reactive power also quickly settles to (0 VAR), confirming proper compensation. In summary, T1-FLC offers balanced and stable regulation with moderate overshoot and fast recovery, making it suitable for smooth operation. IT2-FLC delivers the fastest response and sharpest control action but with higher transient currents and overshoot, which may stress system components. ANN provides robust control with a moderate response and acceptable regulation quality. The choice among these controllers depends on the application's requirements, whether prioritizing speed (IT2-FLC), stability (T1-FLC), or robustness (ANN).]

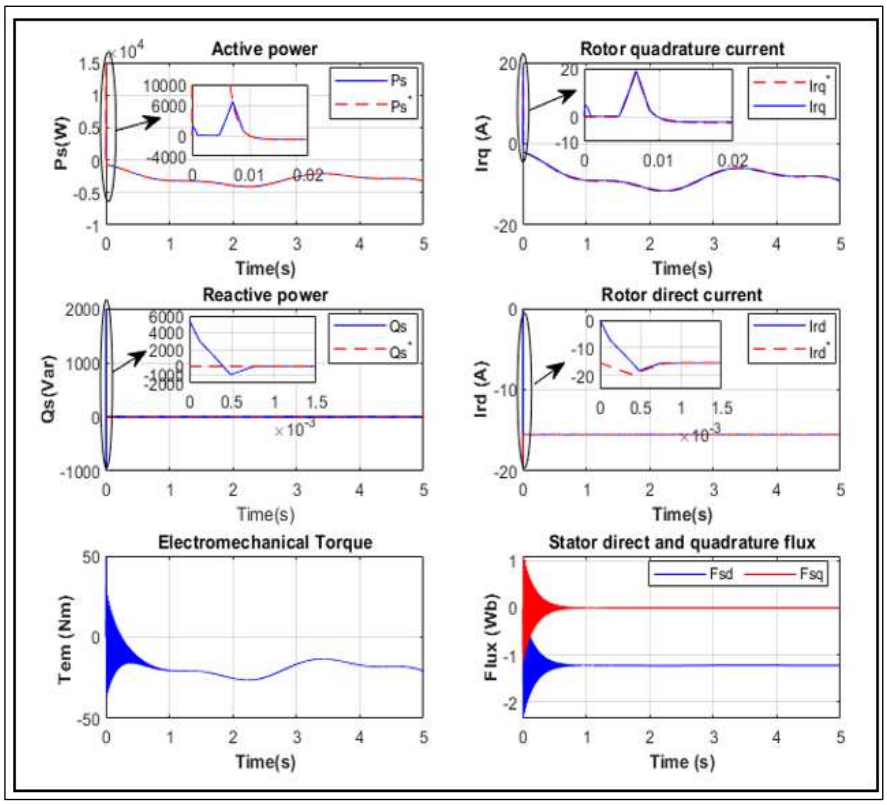

Figure 15: Response of RSC with type 1 fuzzy logic controller.
Source: Authors, (2026).

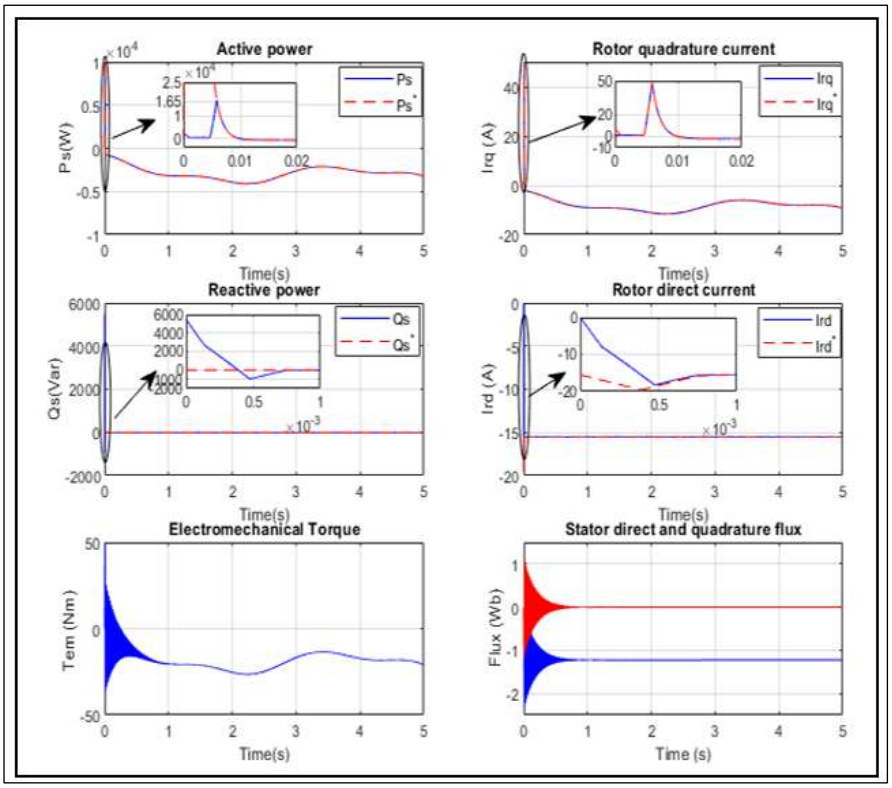

Figure 16: Response of RSC with interval type 2 fuzzy logic controller.
Source: Authors, (2026).

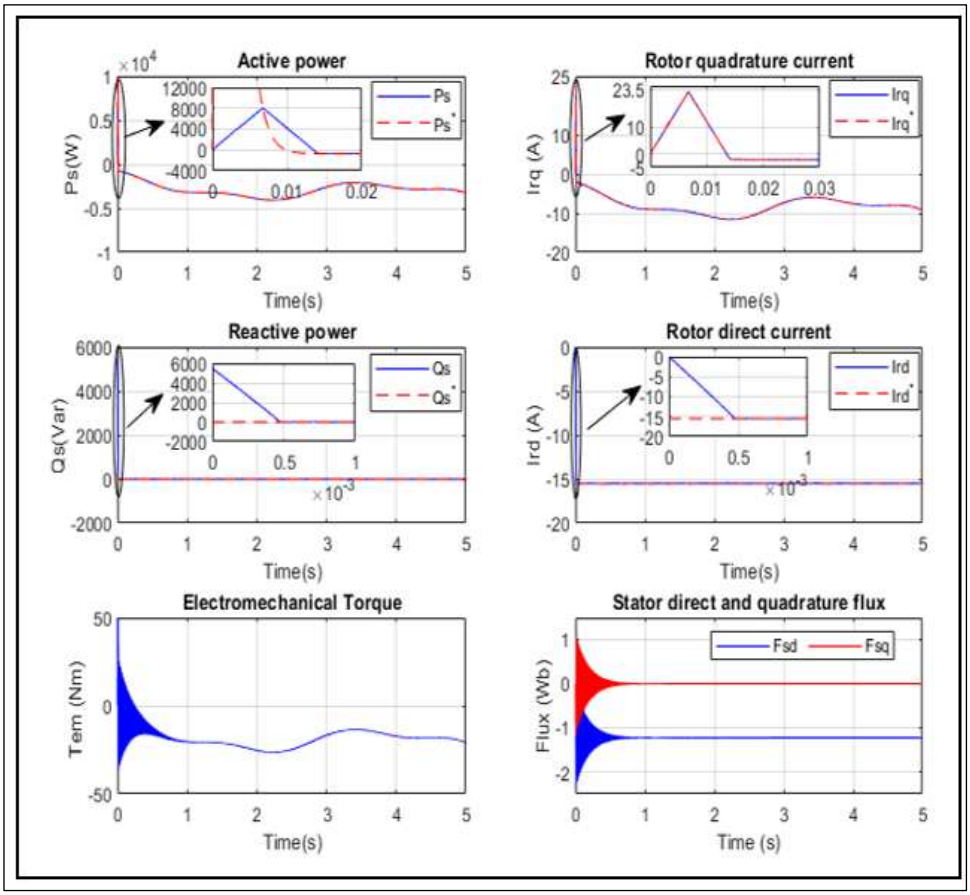

Figure 17: Response of RSC with the ANN controller.
Source: Authors, (2026).

IV.1. QUANTITATIVE COMPARISONS BASED ON ERROR CRITERIA

This test is based on four criteria, which are determined mathematically as follows [6],[21]-[23]. The integral of the squared error (ISE):

$$ISE = \int_0^T e^2(t)\,dt \tag{32}$$

The integral of the absolute value of the error (IAE):

$$IAE = \int_0^T \left|e(t)\right| dt \tag{33}$$

The integral of the time multiplied by the absolute value of the error (ITAE):

$$ITAE = \int_0^T t \cdot \left|e(t)\right| dt \tag{34}$$

The integral of the time multiplied by the value of the squared error (ITSE):

$$ITSE = \int_0^T t \cdot e^2(t)\,dt \tag{35}$$

The criteria are always calculated for a simulation time of Ts = 5 s and power settings equal to those given in the simulation conditions. Table 2 reports a quantitative comparison based on error and time between the proposed control strategies. The results presented in Table 2 show that interval type-2 fuzzy logic control perform the better in terms of minimizing the criteria ISE, IAE, ITAE and ITSE and gives us the lowest values for active and reactive powers and direct and quadrature current, followed respectively by type 1-fuzzy logic control, interval type-2 fuzzy logic control, and artificial neural network.

Table 2: Quantitative comparisons based on error criteria between the developed commands.

G-S	Criterion	Commands Developed for the Considered System		
		T1-FLC	IT2-FLC	ANN
Active powers Ps	ISE	3.811e+8	3.782e+8	3.822e+8
	IAE	1206	1189	1214
	ITAE	62.16	62.14	81.16
	ITSE	5.159e+5	5.084e+5	5.191e+5
Reactive powers Qs	ISE	3328	3229	5104
	IAE	22.24	22.18	30.94
	ITAE	52.77	52.39	74.19
	ITSE	376.1	368.5	668.5
rotor quadrature current Irq	ISE	0.0358	0.0343	0.04318
	IAE	0.06342	0.06335	0.1232
	ITAE	0.148	0.147	0.297
	ITSE	0.002971	0.002917	0.01062
rotor direct current Ird	ISE	0.009932	0.003852	0.01199
	IAE	0.09548	0.08957	0.1087
	ITAE	0.2324	0.2179	0.2679
	ITSE	0.006571	0.005808	0.008872

Source: Authors, (2026).

V. CONCLUSIONS

This study evaluated and contrasted three intelligent control strategies, Type-1 Fuzzy Logic Control (T1-FLC), Interval Type-2 Fuzzy Logic Control (IT2-FLC), and Artificial Neural Networks (ANN), for regulating Doubly Fed Induction Generator (DFIG) based wind turbines. Using a comprehensive system model equipped with MPPT for variable wind speeds, our simulations revealed distinct performance trade-offs. The T1-FLC provided a straightforward control solution with adequate performance under standard operating conditions. In contrast, the ANN controller demonstrated a strong capacity for adaptive learning in response to nonlinear system dynamics; however, its effectiveness is contingent on extensive training data and significant computational power. The IT2-FLC, however, emerged as the superior strategy, offering exceptional robustness against parameter variations and wind turbulence. Its advanced membership structure is uniquely capable of managing and mitigating uncertainty. In summary, IT2-FLC delivered the optimal combination of robustness, precision, and adaptability, establishing it as a highly suitable control method for wind energy applications. Future research will explore hybrid intelligent controllers, specifically the integration of IT2-FLC with advanced nonlinear techniques like second-order sliding mode control, to push performance boundaries further, especially under severe and unpredictable operating scenarios.

VI. AUTHOR'S CONTRIBUTION

Conceptualization: Kouadria Selman, Kouadria Mohamed Abdeldjabbar.
Methodology: Kouadria Selman, Kouadria Mohamed Abdeldjabbar.
Investigation: Kouadria Selman, Kouadria Mohamed Abdeldjabbar.
Discussion of results: Kouadria Selman, and Berkouk El Madjid.
Writing – Original Draft: Kouadria Selman.
Writing – Review and Editing: Kouadria Selman, and Berkouk El Madjid.
Resources: Kouadria Mohamed Abdeldjabbar.
Supervision: Berkouk El Madjid and Rizoug Nassim.
Approval of the final text: Kouadria Selman, Kouadria Mohamed Abdeldjabbar and Berkouk El Madjid.

VII. REFERENCES

[1] C. Óh Aiseadha, G. Quinn, R. Connolly, M. Connolly, W. Soon, "Energy and Climate Policy An Evaluation of Global Climate Change Expenditure 2011–2018", Energies 2020, PP 48-39, 2020. https://doi.org/10.3390/en13184839

[2] M. Flores-Granobles, M. Saeys, "Minimizing CO2 emissions with renewable energy: A comparative study of emerging technologies in the steel industry", Energy & Environmental Science, vol. 13, no 7, p. 1923-1932., 2020. https://doi.org/10.1039/D0EE00787K

[3] S. Ouhssain, H Chojaa, Y. Aljarhizi, E. A. Ibrahmi, A Maarif, M. A. Mossa "Enhancing the Performance of a Wind Turbine Based DFIG Generation System Using an Effective ANFIS Control Technique" International Journal of Robotics and Control Systems Vol. 4, no. 4, 2024, pp. 1617-1640 https://doi.org/10.31763/ijrcs.v4i4.1451

[4] S. Kouadria, Y.Messlem, E. M. Berkouk, "Sliding mode control of the active and reactive power of DFIG for variable-speed wind energy conversion system". In: 3rd International Renewable and Sustainable Energy Conference (IRSEC), 2015, p. 1–8.

[5] S. Kouadria, E. M. Berkouk, Y Messlem and M. Denaï. "Improved control strategy of DFIG-based wind turbines using direct torque and direct power control techniques." Journal of Renewable and Sustainable Energy Vol 10, p 043306, 2018. https://doi.org/10.1063/1.5023739

[6] R. Rouabhi, A. Herizi and A. Djerioui, "Performance of Robust Type-2 Fuzzy Sliding Mode Control Compared to Various Conventional Controls of Doubly-Fed Induction Generator for Wind Power Conversion Systems" Energies, vol 17 no 15, p 3778, 2024. https://doi.org/10.3390/en17153778

[7] A. Milles, E. Merabet, H. Benbouhenni, N. Debdouche, I. Colak "Robust control technique for wind turbine system with interval type-2 fuzzy strategy on a dual star induction generator" Energy Reports Vol 11, 2715–2736, 2024, https://doi.org/10.1016/j.egyr.2024.01.060.

[8] A. V. Hemeyine, A. Abbou, A. Bakouri, M. Mokhlis and S. M. o. M. E. Moustapha "A Robust Interval Type-2 Fuzzy Logic Controller for Variable Speed Wind Turbines Based on a Doubly Fed Induction Generator" Inventions, vol 6, no 21, pp 1-14, 2021, https://doi.org/10.3390/inventions6020021.

[9] S. Shirali, S. Z. Moghaddam, M. Aliasghary "An interval Type-2 fuzzy Fractional-Order PD-PI controller for frequency stabilization of islanded microgrids optimized with CO algorithm" Electrical Power and Energy Systems vol 164, p110422, 2025, https://doi.org/10.1016/j.ijepes.2024.110422.

[10] B. Boudjellal, T. Benslimane "Active and Reactive Powers Control of DFIG Based WECS Using PI Controller and Artificial Neural Network Based Controller" International Information and Engineering Technology Association Vol. 93, no. 1, pp. 31-38, 2020, https://doi.org/10.18280/mmc_a.931-405

[11] M. Hallouz, N. Kabache, S. Moulahoum‡, S. Kouadria "Neural Network Based Field Oriented Control for Doubly-Fed Induction Generator" International Journal of Smart Grid Vol.2, No.3, 2018, https://doi.org/10.20508/ijsmartgrid.v2i3.18.g18

[12] S. Kouadria,; S. Belfedhal,; Y. Messlem,; E. M. Berkouk, "Study and control of wind energy conversion system (WECS) based on the doubly fed induction generator (DFIG) connected to the grid. In: Ninth International Conference on Ecological Vehicles and Renewable Energies (EVER), 2014, p. 1–7.

[13] Saad M. Alwash, Osama Qasim Jumah Al-Thahab , Shamam F. Alwash Modeling and Control Strategies for DFIG in Wind Turbines: A Comparative Analysis of SPWM, THIPWM, and SVPWM Techniques International Information and Engineering Technology Association Vol. 56, no. 6, pp. 963-972, 2023, https://doi.org/10.18280/jesa.560607.

[14] I. Allali, B. Dehiba "A Comparative Study of Interval Type-2 and Type-1 Fuzzy Sliding Mode in Controlling DFIG-Based Wind Energy Conversion System Nigerian Journal of Technological Development, vol. 22, no.3, , pp 101 -110, 2025, *doi:*http://dx.doi.org/10.63746/njtd.v22i3.2818.

[15] K. A. Naika, C. P. Guptab, E. Fernandezb "Design and implementation of interval type-2 fuzzy logic-PI based adaptive controller for DFIG based wind energy system" Electrical Power and Energy Systems vol 115 p 105468, 2020, https://doi.org/10.1016/j.ijepes.2019.105468.

[16] S. G. Bruno, D. E. A. Mansour, A. Nada, T. F. Megahed, "Hybrid ANN-Based MPPT Control for DFIG Wind Systems Using Type-2 Fuzzy Logic and Super-Twisting Sliding Mode Control" Smart Grids and Sustainable Energy, vol. 10, no 2, p. 32, 2025, https://doi.org/10.1007/s40866-025-00261-5.

[17] B. Kaima and A. Boukhelifa, "Output Power Control of a Wind Energy Conversion System Based on a Doubly Fed Induction Generator," International Renewable and Sustainable Energy Conference (IRSEC),.pp. 292– 297, 2013.

[18] E. O. Zouggar, S. Chaouch, D. O. Abdeslam, A. L Abdelhamid" Sliding Control with Fuzzy Type-2 Controller of Wind Energy System Based on Doubly Fed Induction Generator" International Information and Engineering Technology Association Vol. 18, no. 2, pp. 137-146, 2019, https://doi.org/ 10.18280/i2m.180207.

[19]. M. Latha Maheswari, D. Nagarajan, J. Kavikumar, S. Broumi, "Triangular interval type-2 fuzzy soft set and its application". Complex Intell. Syst., vol 6, p 531–544, 2020, https://doi.org/10.1007/s40747-020-00151-6.

[20]. S.K. Raju, G.N. Pillai, "Design and Implementation of Type-2 Fuzzy Logic Controller for DFIG-Based Wind Energy Systems in Distribution Networks". IEEE Trans. Sustain. Energy, Vol 7, p 345–353, 2015., https://doi.org/10.1109/TSTE.2015.2496170.

[21] S. K. Raju, G.N. Pillai "Design and real time implementation of type-2 fuzzy vector control for DFIG based wind generators" Renewable Energy, vol. 88, p. 40-50, 2016, https://doi.org/10.1016/j.renene.2015.11.006.

[22]. M.F. Hamza, H. J. Yap, I.A. Choudhury, "Recent advances on the use of meta-heuristic optimization algorithms to optimize the type-2 fuzzy logic systems in intelligent control". Neural Computing and Applications, vol. 28, no 5, p. 979-999, 2017, https://doi.org/10.1007/s00521-015-2111-9.

[23] R. Rouabhi, A. Zemmit, A. Herizi, O. Moussa, S. Djeriou, "Hybrid type-2 fuzzy backstepping control of doubly fed induction generator for wind energy conversion systems", Journal of the Brazilian Society of Mechanical Sciences and Engineering, vol. 47, no 1, p. 24, 2025, https://doi.org/10.1007/s40430-024-05293-z.

[24] Y. Djeriri, A. Meroufel, et M. Allam, "Artificial neural network-based robust tracking control for doubly fed induction generator used in wind energy conversion systems", J. Adv. Res. Sci. Technol., vol. 2, no 1, p. 173-181, 2015.

[25] B. Azeem et al., "Robust neural network scheme for generator side converter of doubly fed induction generator", in 2017 International Symposium on Recent Advances in Electrical Engineering (RAEE), p. 1-6, 2017.

[26] N. Kabache, S. Moulahoum, K. Sebaa, et H. Houassine, "Neural network-based input output feedback control of induction motor", in Optimization of Electrical and Electronic Equipment (OPTIM), 2012 13th International Conference on, Romania, pp. 578–583, 2012.

[27] Y. Djeriri, "Direct power control based artificial neural networks of doubly fed induction generator for wind energy conversion system application", J. Adv. Res. Sci. Technol., vol. 5, no 1, p. 592–603, 2018.

VIII. APPENDIX

Table 3:Wind Turbine parameters.

Nominal power (P)	10KW
Diameter (D)	3m
Number of blades	3
Gearbox (G)	5.4
Inertial (J)	0.042 kg.m^2
Viscous coefficient (f)	0.017 N.m. s^{-1}

Source: Authors (2026).

Table 4: Doubly Fed Induction Generator parameters.

Nominal power (P)	7.5KW
Nominal voltage (V)	230/380 V
Nominal speed (N)	1500 rpm
Stator resistance (Rs)	0.455 Ω
Rotor resistance (Rr)	0.62 Ω
Stator inductance (Ls)	0.084 H
Rotor inductance (Lr)	0.081 H
Main inductance (Lm)	0.078 H
Pairs of pole number (p)	2
Inertial (J)	0.3125 $Kg.m^2$
Viscous coefficient (f)	$6.73.10^{-3}$ $N.m.s^{-1}$

Source: Authors (2026).